Technical Note TD-07-021

FNAL TD, Aug. 15, 2007

Expected Performance and Test Results of the First Pre-Production Solenoid (Type 2, with Correctors): HINS_CH_SOL_03d

E. Barzi, G. Davis, C. Hess, F. Lewis, D. Orris, M. Tartaglia, I. Terechkine, D. Turrioni, and T. Wokas

I. Solenoid data

To wind the Main Coil, ML-coated SSC inner strand was used, reel # B-2199. Bare strand diameter was 0.808 mm and filament diameter – 6 μm. The strand was coated by the same company that coated the strand for the test coils: MWS Wire Industries. Although we requested single coat, obviously it was heavy coated: the insulated strand diameter is in the range 0.85 – 0.87 mm. This required us to adjust magnetic design slightly to keep the fringe field reasonably low.

The strand performance was measured in the Superconducting R&D laboratory of the Magnet Systems Department at TD and is shown in the table and a graph below:

Table 1: Strand performance:

B (T)	2	3	4	5	6	7	8	9	10
Ic (A)	1176	942	772	629	494	355	235	113	33

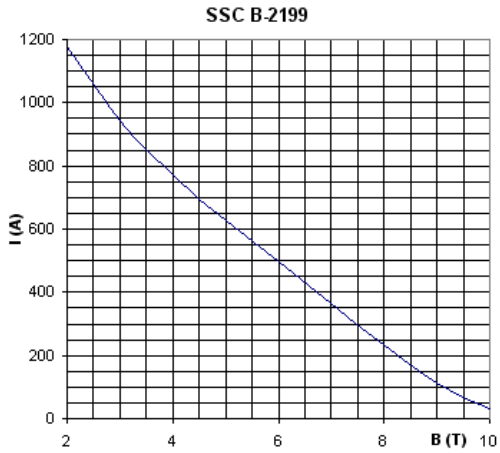

Fig. 1. SSC inner strand (reel B-2199) critical current

The nominal design was based on the use of a strand with outer (insulated) diameter of ~ 0.84 mm and the average compaction factor of ~ 0.75, which was routinely reached during the test coil and the prototype solenoid programs. The corresponding drawing is shown in Fig. 2.

With the new strand we could not reach the planned compaction factor: in the end the average packing of the coil was on the level of ~ 0.716. This has forced us to revisit the magnetic design of the solenoid. New parameters of the main coil are shown below:

Strand Bare diameter = 0.807 mm (Insulated diameter, d = 0.864 mm)

Length, L = 89.1 mm

ID = 64.1 mm

OD = 110.5 mm

Number of wound layers, N_l = 29

The total number of turns, $N_t = 2914$
Compaction Factor K = 2914*0.5115 / 23.25 / 89.1 = 0.721

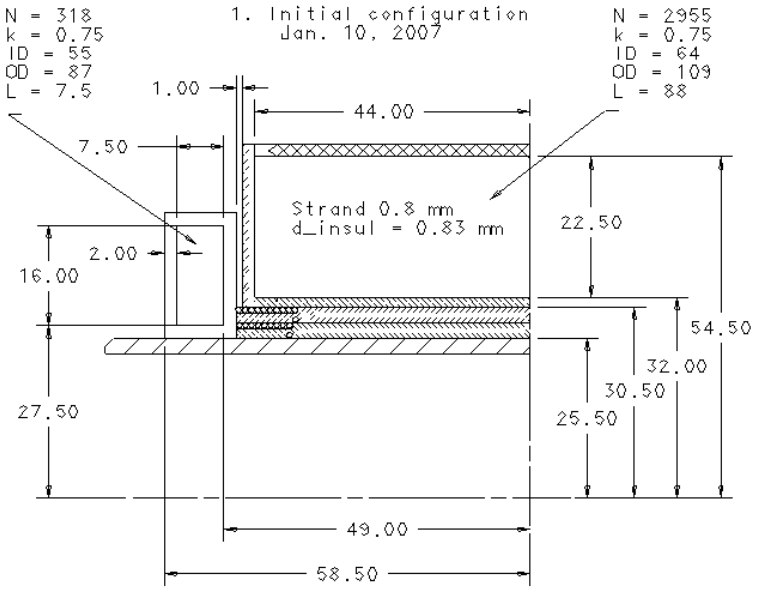

Fig. 2. Nominal design of the solenoid

With the new dimensions and the number of turns in the main coil, some changes in the design of the bucking coil seemed inevitable. The modeling performed to clarify this issue has shown that if the winding pattern of the bucking coil stays as it was anticipated, no corrections are required. But it did not stay. One of major findings during the fabrication was how to keep regular winding patterns during winding the coils. The secret was in adjusting the width of the coil so that it equals an even number of turns in one layer. This was due to the winding technique we used to keep the turns in the adjacent layers "locked" where the transition from one turn to another happens not gradually as it happens during spiral-type winding, but quite locally, at the distance of just several diameters of the strand. The adjustment of the bucking coil design resulted in a new width of the coil, 7.7 mm. The updated solenoid design features are shown in Fig. 3.

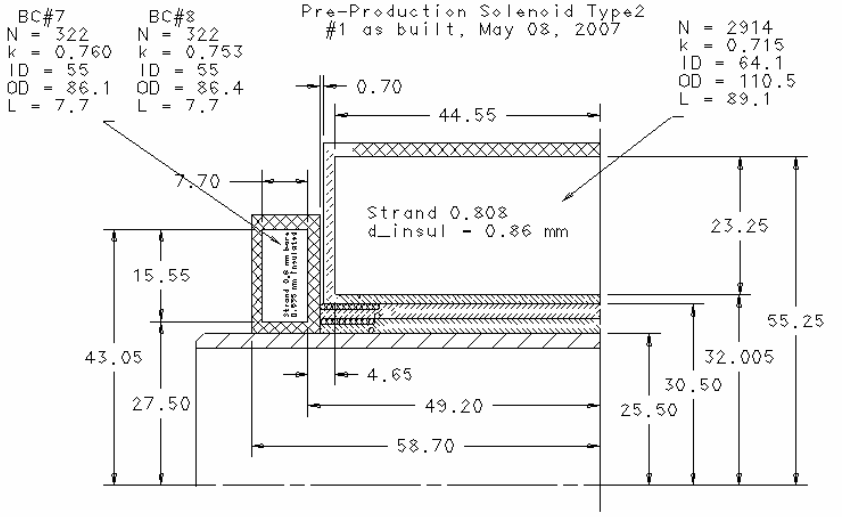

Fig. 3. Modified solenoid design

The bucking coils are wound using the 0.6 mm bare diameter, (0.635 mm coated diameter) NbTi strand made by Oxford. The strand cross-section area S_b= 0.282743 mm^2. Winding parameters of the bucking coil are shown below:

Bucking coil # 7 data:

ID = 55.0 mm
OD = 85.6 - 86.4 mm; (average = 86.0)
L = 7.7 mm
N_t = 322
N_l = 27
K = 0.763
Height per one layer **h**. Coil cross section height **H;** coated strand diameter **d**
$(N_l-1)*h + d = H \rightarrow \mathbf{h} = (H-d) / (N_l-1) = 0.572$

Bucking coil # 8 data:

Strand 0.6 mm bare, 0.635 coated; Sb = 0.282743 mm^2
ID = 55.0 mm
OD = 85.8 - 86.9 mm; (average = 86.5)
L = 7.7 mm
N_t = 322
N_l = 27
K = 0.751
$h = (H-d) / (N_l-1) = 0.560$

II. Correction dipole data

Two corrector windings were each wound in a single layer on concentric cylinders: the inner cylinder was used for the Horizontal Corrector Dipole, which was 90.6 mm in length and had 14 turns; the outer cylinder housed the Vertical corrector Dipole, which was 93.0 mm in length and had 16 turns. Modified by rolling 0.808 mm NbTi strand was used for the coil fabrication. Final strand dimensions were 0.559 x 0.991 bare (0.61 x 1.01 insulated). A short section of one strand in the horizontal corrector was flattened too much, and it was thought to be possibly damaged (see Figure 7), so this section was mechanically supported by splicing another piece of strand to it; in fact this did not impact the quench performance of the coil.

III. Test Overview

The cold test took two days: Thursday 6/14 and Friday 6/15. A thermal history of the test is shown in Fig. 4. The bath temperature during quench testing varied from 4.22 to 4.24 K. Data acquisition, power, and protection systems described in previous test notes were adapted for use in this test with minor modifications for the voltage tap configuration.

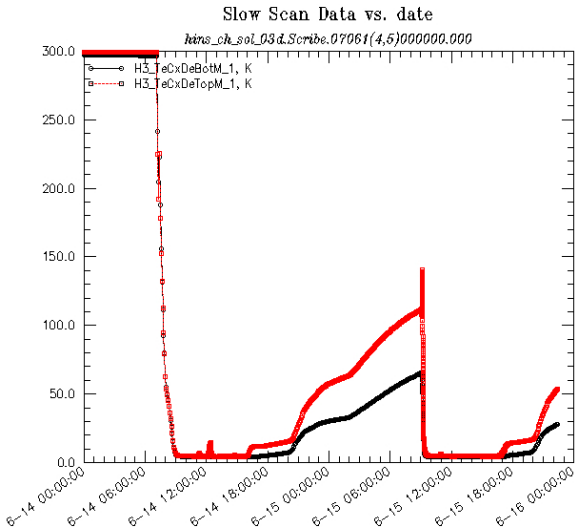

Fig. 4. Thermal history of HINS_CH_SOL_03d cold test

IV. Quench Protection and Solenoid Performance

The predicted quench current occurs where the calculated magnet load line crosses the strand critical surface (from Table 1). The behavior of the magnetic field with current is slightly non-linear due to magnetization of the soft iron yoke, so modeling has been done at different currents for comparison to test data (using COMSOLE software vendor-supplied μ vs H data). The magnetic field map with the "nominal" bucking coils (7.5 mm length, 16 mm height, 318 turns) at 221 A (first approximation to the quench current) is shown in Fig. 5. Load Curve is shown in Fig. 6 below

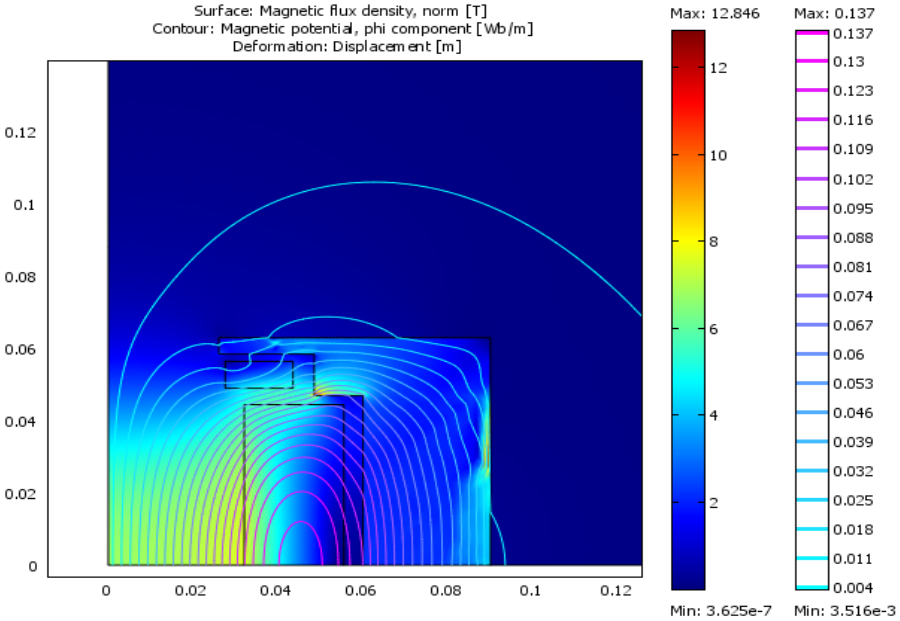

Fig. 5. Field map at 221 A

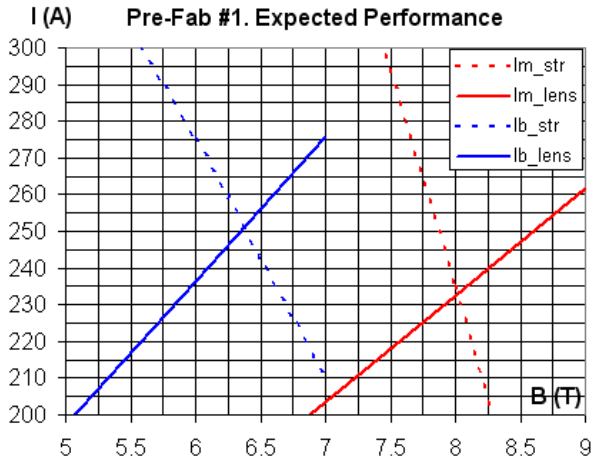

Fig. 6. Load Diagram for as-built HINS_CH_SOL_03d.

The expected quench current for the main coil is 233 A. At this current the magnetic field in the center of the solenoid is B_c= 7.06T, and maximum field on the coil is B_m= 8T. The Focusing Field Integral at the quench current is B^2* dl = 331 T^2-cm. The requirement of 200 T^2-cm is met at 180 A, thus predicting a current margin of ~ 30 %.

The recommended and implemented connection scheme is shown in Fig 7. The main coil in the solenoid did not have a central tap. Taps around each coil were added outside of the solenoid. Protection was initiated based on the total voltage across the solenoid. Additional taps between the coils in the solenoid were added for quench characterization. A dump resistor, R = 0.6 Ohm, was used, although modeling shows the solenoid is safe if all the stored energy (at maximum current) dissipates inside. After quench detection the power supply was immediately shutting down.

The corrector windings were connected in series and a voltage tap was added between the coils. An additional power lead was added between the vertical and the horizontal dipole so that they could be tested separately (they have slightly different properties). Additional taps around the dipoles were added for quench characterization. No dump resistor was needed for the corrector protection (this feature does not help here). Power supply was shutting down immediately after quench detection: the correctors can be irreversibly damaged otherwise.

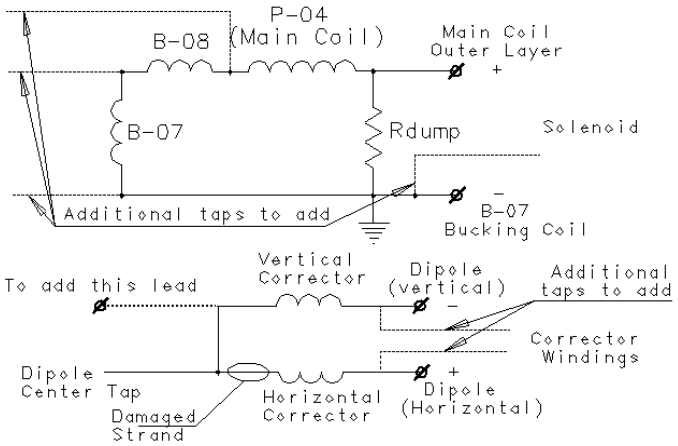

Fig. 7. As-built connection scheme

The ramp history from the Lakeshore power supply, used for the main and bucking coils is shown in Fig. 8. (Note that the peak recorded currents here are slightly below the achieved level, because after quenching the current quickly goes down and slow scan captures data every 2-3 seconds). Unfortunately, no history of the corrector dipole current was recorded, as there is no signal from the trim power supply to digitize.

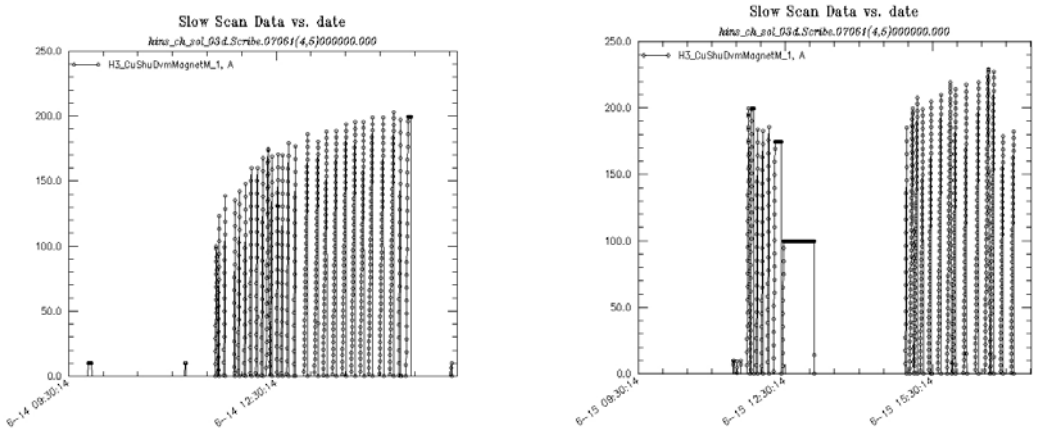

Fig. 8. Ramp history for the two-day quench training and magnetic measurement test.

IV.1) Initial Solenoid Training

Initial ramp rate was 2 A/s with brief delays between ramps. Training was quite slow. The first quench started at 130 A and it took 25 cycles to reach 200 A. Mainly the quenches occurred in the main coil, but quenches # 2 and #17 were located in the bucking coil #8. Several times a spike precursor was noticed before quench developed. After the spike, the next quench current was usually lower, but continued to rise later. Switching to the 1A/s ramp rate with longer delays between ramps seemed to result in more rapid training.

IV.2) Corrector Coil Training

The solenoid was ramped to 200 A and training of the correctors in the solenoid field was initiated. However, quenches **in the bucking coil #8** did not allow us to use 200 A for the training, so the solenoid current was set to 175 A. At 175 A in the solenoid, it was possible to increase the current in the correctors (in series) up to 278 A, which was the limit of the power supply.

IV.3) Final Solenoid Training

After the correctors were tested, the solenoid training cycle could be finished. It took 13 cycles with 1A/s ramp rate to bring the current to the level of ~232 A, which is quite close to the expected quench current 233 A. During this training, quenches occurred both in the main coil and in bucking coil #8. However, after initiating manual trip at 232 A, we could not get back to the same level of the current, reaching only 184 A due top quenching in the bucking coil #8. After two attempts, suspecting a turn-to-turn short, we stopped the training.

V. Magnetic Field

V.1) Magnetic Field in the Solenoid

Magnetic measurements of the solenoid were made at a current level of 100 A. The predicted magnetic field distribution along the axis of the solenoid is shown in Fig. 9, and the measured profile is shown in Fig. 10; the two graphs (that almost overlap) correspond to the data taken manually and by using automated data acquisition system (in which position and field measurements are not exactly synchronized). The predicted peak strength is about 2% below the measured value, and the shapes are quite similar.

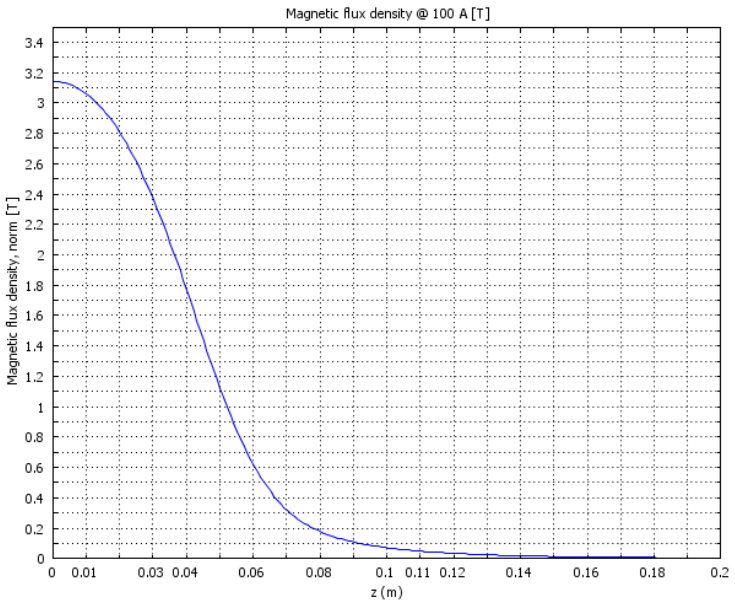

Fig. 9. Predicted Magnetic field profile along the axis at I = 100 A.

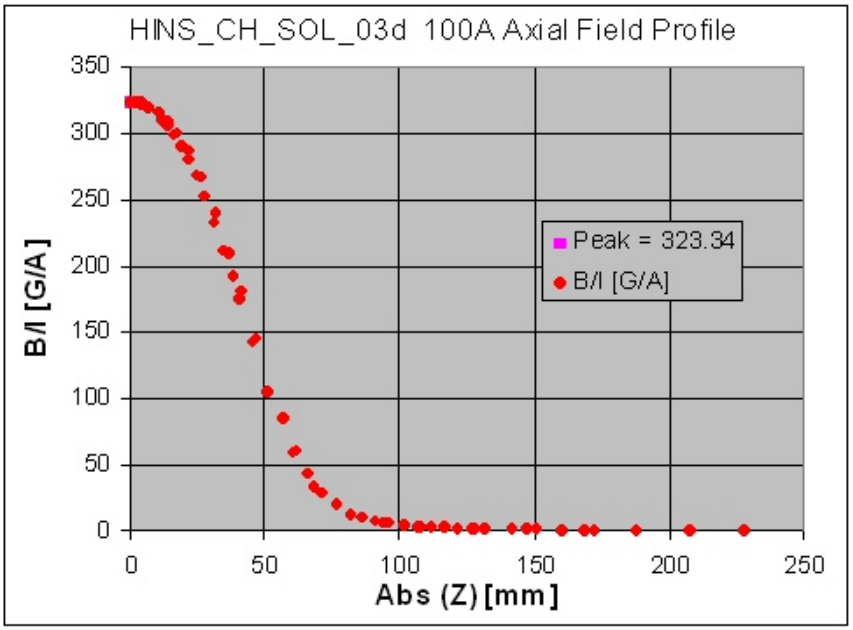

Fig. 10. Measured magnetic field profile along the axis at I=100 A.

The field far from the solenoid center is interesting, of course, in terms of the bucking coil effectiveness. Figure 11 shows the measured profile in the tail: it is quite symmetric in this solenoid.

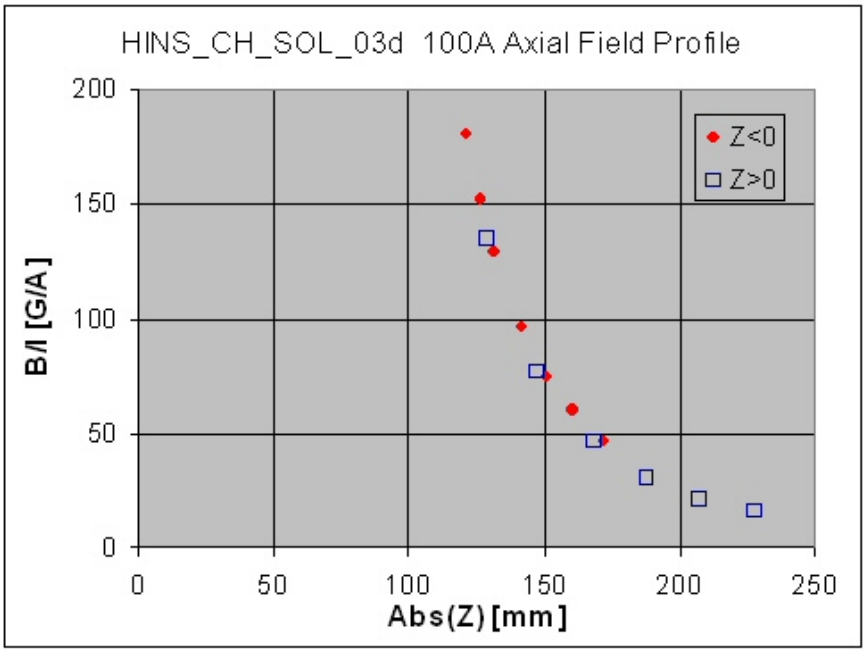

Fig. 11. Measured fringe magnetic field along the axis at 100 A

The yoke design intentionally introduces a small (~0.45 mm warm, 0.3 mm cold) gap between the two halves of the flux return, at the solenoid center, for the control of forces in the magnet. Fig. 12 shows the predicted tail profile with a gap, and Fig. 13 shows the no-gap case: the fringe field on axis becomes lower with the gap. In both cases, the measured field is lower than the predicted value. This issue will require additional study and can be a result of using non-adequate steel permeability approximation during modeling.

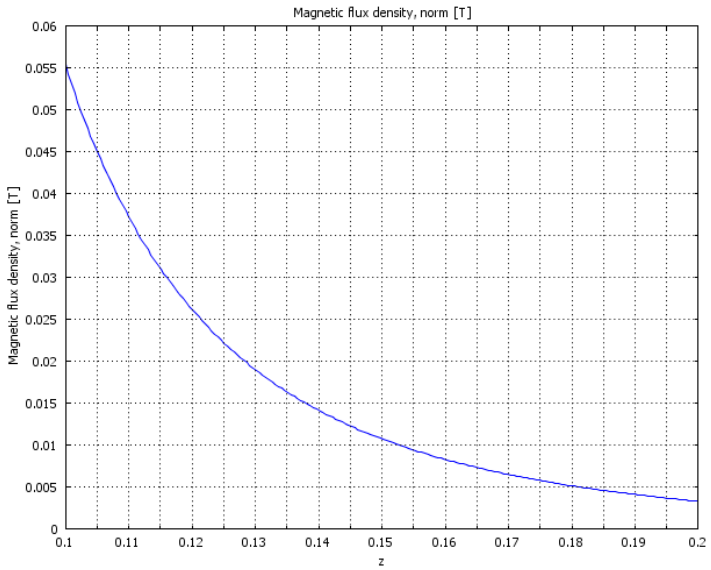

Fig. 12. Tail magnetic field outside the solenoid (with 0.3 mm gap) at I = 100 A

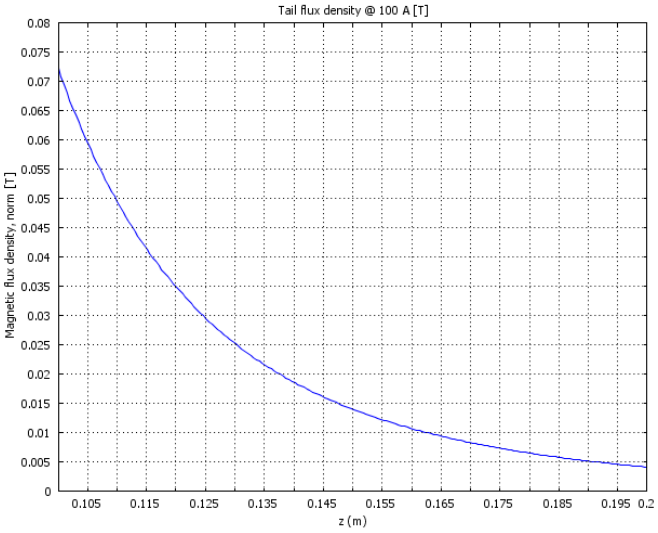

Fig. 13. Predicted magnetic field tail (outside the solenoid) with no gap in the flux return at I = 100 A

It is quite interesting observation that adding a gap really helps to reduce fringe magnetic field on the axis. This fact also needs to be studies.

The Magnetic Field distribution along the radius at Z = 0 mm (in the center of the magnet) is shown in Fig. 14, and at Z = 150 (outside the magnet) in Fig 15 for I = 220 A. These distributions were not measured during the test. Inside the magnet the magnetic field is ~ 11% lower than it is on the inner layer of the winding. Outside the magnet, at the distance 150 mm from the center, the magnetic field has maximum on the axis.

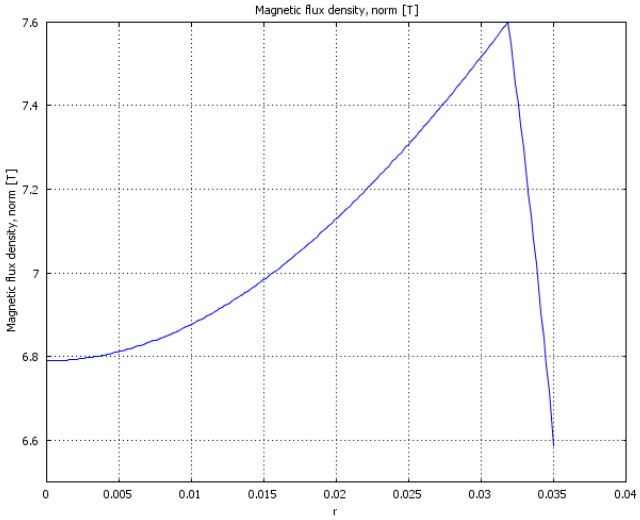

Fig. 14. Magnetic field in the transverse central plane (I = 220 A)

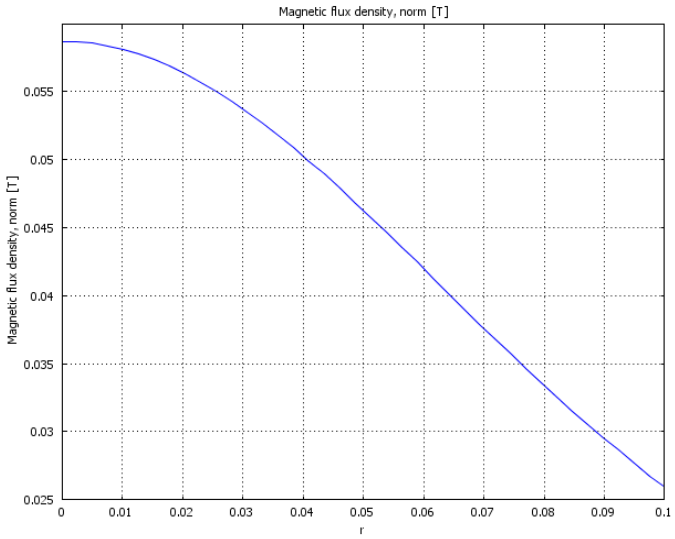

Fig. 15. Magnetic field in the transverse plane 150 mm from the center (I = 220 A)

V.2) Magnetic Field in the Dipole Correctors

Expected performance of the correctors was discussed in [1], although at that stage number of turns in the correctors was a bit different: 18 for the horizontal corrector (inner) and 20 for the vertical corrector (outer). Radii of the correctors also differed slightly from that of the latest version of the design. Fig. 16, reproduced from [1], shows the calculated distribution of the magnetic strength (in the dipole direction) along lines parallel to the axis in the horizontal dipole, for I = 250 A. The field is quite uniform in the central part of the solenoid, and its integral along the axis is 0.51 T-cm. The required integrated strength is 0.25 T-cm for this type of solenoids, which is reached at I ≈ 125 A.

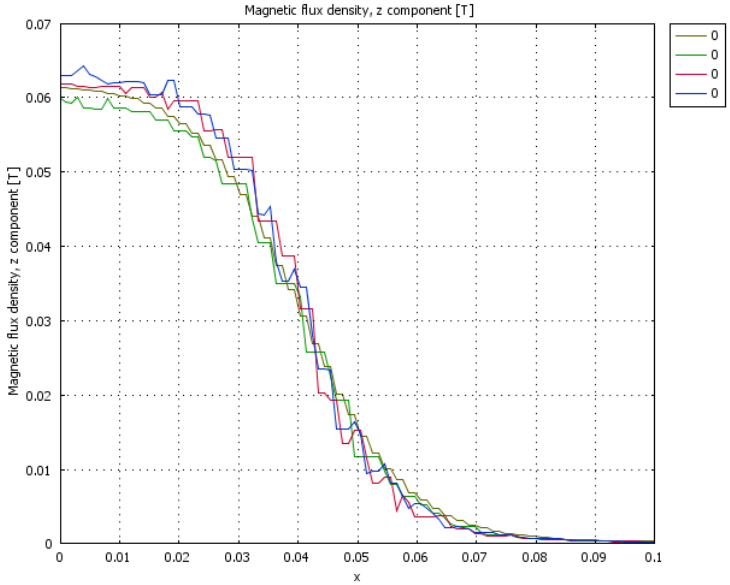

Fig. 16. Vertical magnetic field profile for the horizontal corrector at I=250 A along several lines parallel to the solenoid axis, at differing azimuth and radius (from [1]).

Measurement of the horizontal and vertical corrector field profiles were conducted using 1-D Hall probe at I = 200 A. The horizontal dipole profile is shown in Fig. 17; the vertical dipole profile is in Fig. 18. Comparison of the measured and modeled field distributions, considering the differences in number of turns, show good agreement. The measured profiles give integrated strength values shown in Table 2.

Table 2. Integrated B*dl dipole corrector strengths for HINS_CH_SOL_03d

	B/I*dl [G-m/A]	B*dl at 125 A [T-cm]	B*dl at 200 A [T-cm]
H dipole	.2076	.2329	.3726
V dipole	.1863	.2595	.4152

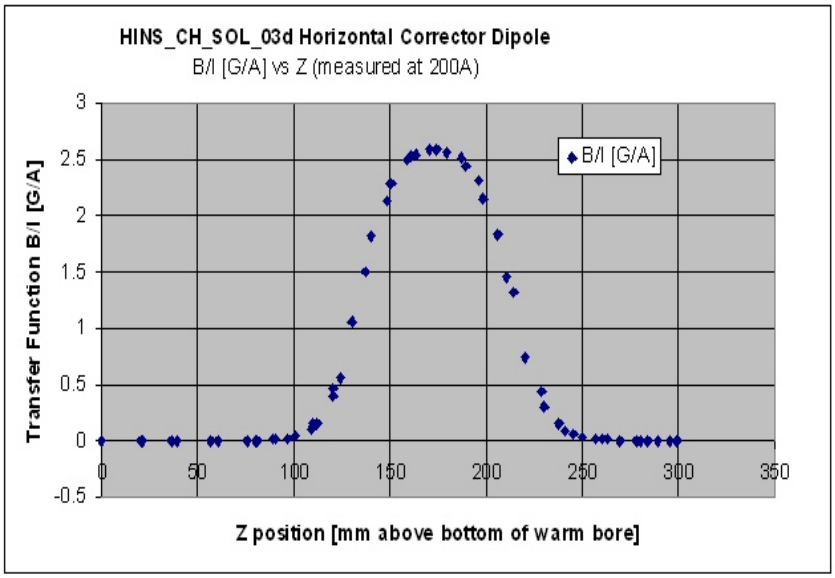

Fig. 17. Magnetic field profile of the horizontal corrector

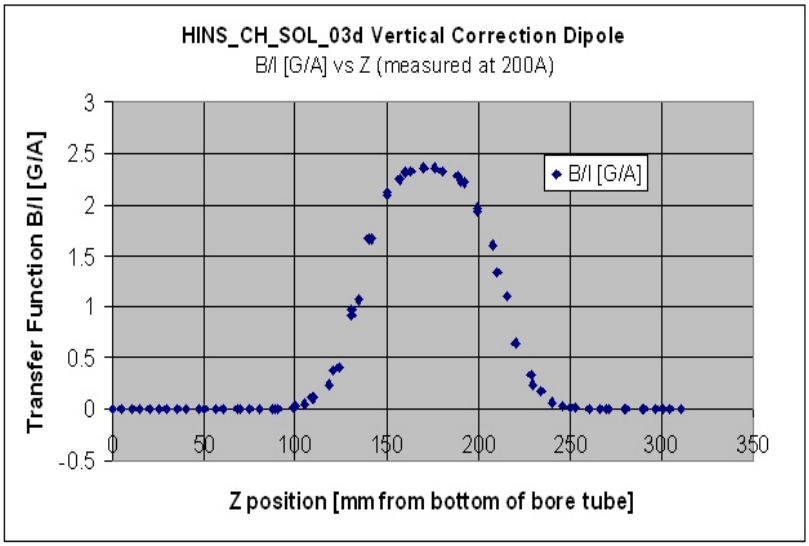

Fig. 18. Magnetic field profile of the vertical corrector at 200 A

VI. Conclusion

1. Although the solenoid reached predicted maximal current, unusually long training and slip back in the quench current will require additional attention. Initially we thought that layer-to-layer resistance somewhere in the bucking coil winding could be responsible for the anomalous behavior. Cold ring test (using LN2 bath) did not provide an evidence for this effect though. Further study is needed here.
2. Corrector windings proved to be quite robust and will provide needed beam steering.
3. Test setup of the next pre-production solenoid must provide more flexibility to allow separate training of bucking coils.

References:

1. G. Davis, V.V. Kashikhin, T. Page, I. Terechkine, T. Wokas, Linac CH-type Cavity Section Focusing Solenoid Cold Mass Design, FNAL, TD-06-020, Apr. 2006.
2. G. Davis, I. Terechkine, T. Wokas, CH-Section Focusing Solenoid with Dipole Corrector Windings, FNAL, TD-07-001, Jan. 2007.